

<sup>6</sup>K. T. Knöpfle, H. Riedesel, K. Schindler, G. J. Wagner, C. Mayer-Böricke, W. Oelert, M. Rogge, and R. Turek, in Proceedings of the International Conference on Nuclear Interactions, Canberra, Australia, 1978, edited by B. A. Robson (Springer, Heidelberg, to be published), and to be published.

<sup>7</sup>P. D. Kunz, code DWUCK4 (unpublished).

<sup>8</sup>D. H. Youngblood, J. M. Moss, C. M. Rozsa, J. D. Bronson, A. D. Bacher, and D. R. Brown, Phys. Rev. C **13**, 994 (1976).

<sup>9</sup>C. C. Chang, F. E. Bertrand, and D. C. Kocher, Phys. Rev. Lett. **34**, 221 (1975).

<sup>10</sup>R. Stokstad, Code STATIS (unpublished).

<sup>11</sup>Because of the difficulties discussed in the next two paragraphs, it is very difficult to determine the angu-

lar correlation of the GQR decay to a particular final state. However, the angular correlation of the GQR and underlying continuum to all final states (limited statistics prevent a reliable background subtraction) is indistinguishable from that of the adjacent continuum.

<sup>12</sup>T. Yamagata, K. Iwamoto, S. Kishimoto, B. Saeki, K. Yuasa, M. Tanaka, T. Fukuda, K. Okada, I. Miura, M. Inoue, and H. Ogata, Phys. Rev. Lett. **40**, 1628 (1978).

<sup>13</sup>A. Moalem, W. Benenson, G. M. Crawley, and T. L. Khoo, Phys. Lett. **61B**, 167 (1976); A. Moalem, Nucl. Phys. **A281**, 461 (1977).

<sup>14</sup>L. Meyer-Schützmeister, R. E. Segel, K. Raghunathan, P. T. Debevec, W. R. Wharton, L. L. Rutledge, and T. R. Ophel, Phys. Rev. C **17**, 56 (1978).

## Electron Scattering from the Ground-State Magnetization Distribution of $^{17}\text{O}$

M. V. Hynes, H. Miska,<sup>(a)</sup> B. Norum, W. Bertozzi, S. Kowalski,  
F. N. Rad, C. P. Sargent, T. Sasanuma, and W. Turchinetz

*Department of Physics, Laboratory for Nuclear Science, Massachusetts Institute of Technology,  
Cambridge, Massachusetts 02139*

and

B. L. Berman

*Lawrence Livermore Laboratory, University of California, Livermore, California 94550*

(Received 30 May 1978)

Elastic electron scattering has been used to determine the transverse form factor of the  $^{17}\text{O}$  ground state in the effective momentum-transfer range  $0.55 \leq q_e \leq 2.8 \text{ fm}^{-1}$ . The data show considerable deviation from single-particle predictions; in particular, a sizable suppression of the  $M3$  and an enhancement of the high- $q$  side of the  $M5$ . Recent shell-model, core-polarization, and meson-exchange calculations are not adequate to explain these effects.

We report here the first measurements of elastic electron scattering from the magnetization density of  $^{17}\text{O}$ . The static magnetic dipole moment ( $-1.894 \text{ nm}$ )<sup>1</sup> being very close to the Schmidt limit ( $-1.913 \text{ nm}$ ) has been viewed as strong evidence for the single-particle nature of this nucleus. In addition, the spectroscopic factor for the  $d_{5/2}$  single-particle component of the ground state as determined by  $(d, p)$  reactions is about 0.9.<sup>1</sup> However, the existence of a sizable quadrupole moment ( $-2.562 e\text{-fm}^2$ )<sup>1</sup> for the ground state of  $^{17}\text{O}$  and the large  $E2$  strengths connecting the ground state to the  $\frac{1}{2}^+$  (0.871 MeV) and  $\frac{3}{2}^+$  (5.083 MeV) states indicate a limit to the usefulness of the extreme single-particle model for this nucleus. These effects can be viewed as due to the nonspherical structure of the  $^{16}\text{O}$  core and its polarization by the odd neutron. Under these circumstances, the  $^{16}\text{O}$  core is expected to in-

fluence the magnetization of  $^{17}\text{O}$ . Electron scattering determines the spatial distribution of the magnetization density and hence provides a severe test of our understanding of the structure of  $^{17}\text{O}$ .

The data were collected at the Massachusetts Institute of Technology-Bates Linear Accelerator using the high-resolution energy-loss spectrometer system.<sup>2</sup> Scattered-electron spectra were measured at three scattering angles,  $90^\circ$ ,  $160^\circ$ ,<sup>3</sup> and  $180^\circ$ .<sup>4</sup> The three  $^{17}\text{O}$  targets used were isotopically enriched BeO foils manufactured at Lawrence Livermore Laboratory.<sup>5</sup> The  $^{17}\text{O}$  isotopic enrichments ranged from about 20 to 85%. Target thicknesses ranged from about 20 to 40 mg/cm<sup>2</sup>. Normalization for most of the  $^{17}\text{O}$  data at each energy was relative to  $^{16}\text{O}$ . For the two highest energy points at  $160^\circ$ , where the  $^{16}\text{O}$  cross section was prohibitively small, normalization

was relative to  ${}^9\text{Be}$ . The  ${}^9\text{Be}$  cross section was determined in a separate exposure of a pure  ${}^9\text{Be}$  metal foil. For the  $180^\circ$  data, the cross sections were determined using the geometrical constants of our system. The  ${}^9\text{Be}$  cross sections determined at  $180^\circ$  in this way agree with measurements from other laboratories.<sup>6</sup>

The electron-scattering cross section can be written in first Born approximation as

$$\frac{d\sigma}{d\Omega} = \frac{Z^2\sigma_M}{\eta} [ |F_L(q)|^2 + \left\{ \frac{1}{2} + \tan^2\left(\frac{1}{2}\theta\right) \right\} |F_T(q)|^2 ],$$

where  $Z$  is the atomic number of the target nucleus,  $\sigma_M = \alpha^2 \cos^2(\frac{1}{2}\theta) / 4E_0^2 \sin^4(\frac{1}{2}\theta)$  is the Mott cross section,  $\alpha$  is the fine structure constant,  $\theta$  is the scattering angle,  $E_0$  is the incident energy,  $\eta = 1 + (2E_0/M) \sin^2(\frac{1}{2}\theta)$  is the recoil factor,  $M$  is the mass of the target nucleus,  $q = (2E_0/\eta^{1/2}) \sin\frac{1}{2}\theta$  is the momentum transfer, and  $F_L$  and  $F_T$  are the longitudinal and transverse form factors, respectively.

A comparison of the plane-wave Born-approximation result and a magnetic distorted-wave Born-approximation (DWBA) calculation was made in order to account for the effects of Coulomb distortion. We have varied the factor  $f$  in the effective- $q$  transformation,  $q_{\text{eff}} = q(1 + fZ\alpha/RE_0) \equiv q_\epsilon$ , where  $R^2 = \frac{5}{3} \langle r^2 \rangle$  and  $\langle r^2 \rangle^{1/2}$  is the rms charge radius of the target nucleus. Excellent overlap with plane-wave Born-approximation form factors is obtained when DWBA form factors are transformed to  $q_{\text{eff}}$  with  $f = 1.09$ . Accordingly, the data presented here are plotted at  $q_{\text{eff}}$ .

The experimental results for the square of the transverse form factor for  ${}^{17}\text{O}$  are shown in Fig. 1. These form factors were extracted from the measured cross sections using the Rosenbluth method, in which the data points at  $160^\circ$  and  $90^\circ$  were matched at the same values for  $q_{\text{eff}}$ . For the  $180^\circ$  points, the transverse form factor was extracted by using measurements of the charge contributions to the cross section (due to finite solid angle) from a separate exposure of a BeO foil with the natural  ${}^{16}\text{O}$  abundance, taking into account our precise knowledge of the charge-scattering cross-section ratio for  ${}^{17}\text{O}$  to  ${}^{16}\text{O}$ .<sup>3</sup> The charge-scattering contributions at  $180^\circ$  were in general small, the largest being 60% for the measurement at  $q_\epsilon = 0.55 \text{ fm}^{-1}$ .

The ground-state spin and parity assignment for  ${}^{17}\text{O}$  is  $\frac{5}{2}^+$ . Thus, in elastic scattering the allowed transverse multipoles are  $M1$ ,  $M3$ , and  $M5$ . We have calculated the contributions of these

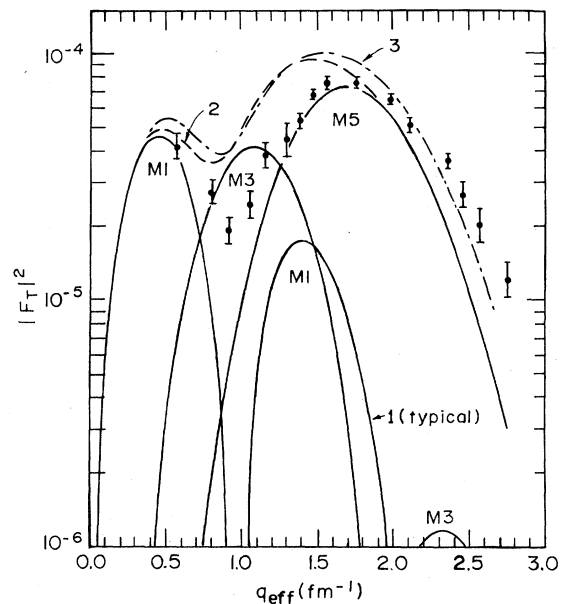


FIG. 1.  ${}^{17}\text{O}$  transverse form factor data. Curves indicate results of single-particle calculations using HO wave functions. Curve 1, individual multipoles ( $b = 1.8 \text{ fm}$ ); curve 2, total form factor for  $b = 1.8 \text{ fm}$ ; and curve 3, total form factor for  $b = 1.7 \text{ fm}$ .

multipoles in the context of the strict single-particle model. The curves displayed in Fig. 1 result from such a calculation using harmonic-oscillator wave functions for a  $d_{5/2}$  neutron outside an inert  ${}^{16}\text{O}$  core. From our charge-scattering measurements<sup>3</sup> we have determined that the oscillator parameter  $b$  appropriate for the  ${}^{17}\text{O}$  charge distribution is approximately  $1.80 \text{ fm}$ . The solid curves in the figure indicate the individual multipole contributions for this oscillator parameter, while the broken curves indicate their sum for this and for  $b = 1.7 \text{ fm}$ . Corrections for center-of-mass motion and finite nucleus size have been applied.<sup>7</sup> It is evident that the data deviate significantly from these single-particle predictions. For  $0.5 \leq q_\epsilon \leq 1.75 \text{ fm}^{-1}$  the data lie considerably below the single-particle prediction, thus indicating a sizable suppression of the  $M3$  multipole. For  $2.0 \leq q_\epsilon \leq 2.8 \text{ fm}^{-1}$  the data stand appreciably above the calculation.

In order to compare the data with a more realistic single-particle calculation, the transverse form factor was evaluated using a Woods-Saxon (WS) wave function.<sup>8</sup> The well depth and spin-orbit strength were fixed by fitting energy levels in  ${}^{15}\text{N}$ ,  ${}^{15}\text{O}$ ,  ${}^{17}\text{O}$ , and  ${}^{17}\text{F}$ . The well radius was determined by requiring that the elastic electron-scattering cross section from  ${}^{16}\text{O}$  be reproduced.

Center-of-mass and finite-nucleon-size corrections have been applied with the assumption that they are the same as those for a harmonic oscillator (HO) with  $b = 1.77$  fm. It is evident that the result of this WS calculation, shown in Fig. 2(a), does not fit the data.

The deviations in both shape and magnitude between the data and these single-particle calculations suggest a more complicated structure for the  $^{17}\text{O}$  ground state. In fact, the static quadrupole moment requires the participation of the  $^{16}\text{O}$  core. In order to account for this effect, some theories include multiparticle, multihole excitations of the core in shell-model calculations with the one-particle, one-hole (1p-1h) excitations represented by an effective charge. Unfortunately, the concept of effective charge is not appropriate for our purposes, where currents and the momentum dependence of amplitudes are relevant. The influence of the multiparticle, multihole structure of the  $^{16}\text{O}$  core can still be estimated

using these shell-model calculations without effective charges. In order to include these effects we have used the transition densities for  $^{17}\text{O}$  as obtained from the Michigan State University (MSU) shell-model calculations, to evaluate the  $M1$ ,  $M3$ , and  $M5$  multipoles. In this calculation, the complete  $1p_{1/2}$ ,  $2s_{1/2}$ , and  $1d_{5/2}$  shells were active.<sup>9</sup> These results are displayed using HO wave functions ( $b = 1.80$  fm) in Fig. 2(b). Except for the region where  $M1$  dominates, they show a small uniform suppression of the total form factor relative to the single-particle value. In particular, since the data in the region where the  $M5$  is dominant are higher than even the single-particle value, it is clear that multiparticle, multihole excitations of this limited scope are not by themselves sufficient to explain the data.

Recently, Arima *et al.*<sup>10</sup> have calculated the transverse form factor for  $^{17}\text{O}$  including core-polarization effects via 1p-1h excitations (up to  $6\hbar\omega$ ) with a Rosenfeld effective interaction. Also calculated were the two-body exchange-current contributions including both pionic and pair terms in the nonrelativistic one-pion-exchange potential. A calculation by Dubach<sup>11</sup> for  $^{17}\text{O}$  has shown that inclusion of the isobar has negligible effect for the range of momentum transfer of interest here. The results of Arima *et al.*, both with and without exchange-current effects, are displayed in Fig. 2(c). For  $q_e \sim 0.5$  fm $^{-1}$ , near the first peak of the  $M1$ , the core polarization depresses the form factor slightly. However, the exchange-current effects here restore the form factor to nearly its full single-particle value. For  $0.6 \leq q_e \leq 1.5$  fm $^{-1}$  core polarization suppresses the total form factor considerably, while exchange effects raise it back up only slightly. Most of the suppression in this region comes from a reduction of the  $M3$  cross section by about a factor of 3 at the peak. However, this suppression is in part defeated by an increase of the second lobe of the  $M1$  by a factor of about 2 at its peak. The  $M5$  cross section is not substantially changed. The net result gives a poor final fit to the data in this region. For  $2.0 \leq q_e \leq 3.0$  fm $^{-1}$ , where the  $M5$  is dominant, core polarization gives a very slight enhancement of the form factor, while the exchange-current contributions produce a nearly constant overall enhancement. In this region the slope of the experimental form factor is not reproduced by this calculation. Other core-polarization calculations by Zamick<sup>12</sup> and Brown<sup>13</sup> for  $q = 0$  show  $M3$  suppression as well.

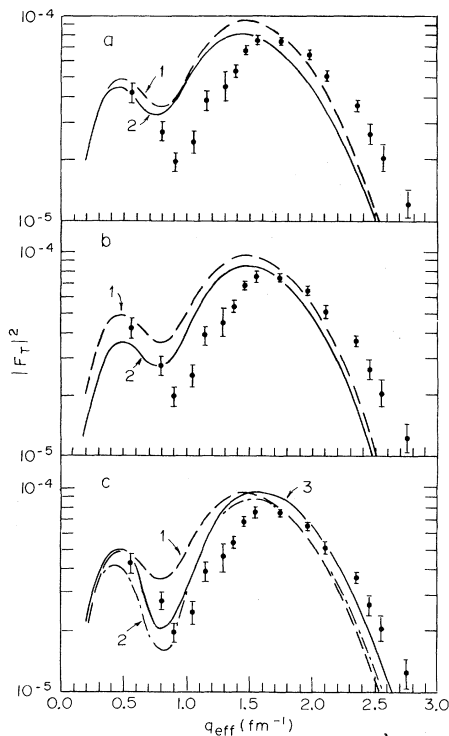


FIG. 2. Comparison of data with various theoretical calculations for  $^{17}\text{O}$  transverse form factor. (a) Curve 1, HO ( $b = 1.8$  fm); curve 2, WS calculation. (b) Curve 1, HO ( $b = 1.8$  fm); curve 2, MSU shell model. (c) Curve 1, HO ( $b = 1.8$  fm); curve 2, HO + core-polarization effects; curve 3, HO + core-polarization +  $\pi$ -exchange effects.

In order to give a better picture for this nucleus, the results of shell-model calculations for  $^{17}\text{O}$  should be combined with core-polarization and meson-exchange calculations. However, it is likely that agreement with experiment for  $0.6 \leq q_\epsilon \leq 1.5 \text{ fm}^{-1}$  still would be inadequate, and for  $2.0 \leq q_\epsilon \leq 3.0 \text{ fm}^{-1}$ , such a combination of effects will do nothing to change the slope of the form factor as required by the data.

In an odd-even nucleus with the odd nucleon in a stretched single-particle configuration ( $J_0 = l + \frac{1}{2}$ ) and with a spin  $J_0$  that is larger than those of the filled shells, the cross section for the magnetic multipole  $M\lambda$  with  $\lambda = 2J_0$  is considered to be determined almost exclusively by the radial wave function of the unpaired nucleon. The influence of core excitation on this multipole is expected to be very small since multiparticle effects of low-energy origin (i.e.,  $2p$ - $2h$  excitations of  $1\hbar\omega$ ) cannot contribute because of angular momentum conservation.<sup>14</sup> Since the high- $q$  part of the magnetic form factor is thought to be dominated by the highest multipole, some authors have used the single-particle character of this multipole to justify a determination of the radius of the last nucleon orbital from appropriate experimental data.<sup>15</sup> In the case of  $^{17}\text{O}$ , fitting the data by varying the radius of the nucleon potential would be equivalent to a decrease in the radius of the  $d_{5/2}$  neutron orbital by roughly 10% for both the WS and HO( $b = 1.8 \text{ fm}$ ) cases presented earlier. This effect is nearly halved by the corrections for meson exchange. The uncertainties in these corrections, as well as the uncertainties in the qualitative first-order justification for the single-particle nature of the  $M5$  multipole, render such an interpretation very speculative at this time.

In conclusion, the data we have presented show a strong suppression of the  $^{17}\text{O}$  magnetic form factor for the momentum transfer region  $0.75 \leq q_\epsilon \leq 1.6 \text{ fm}^{-1}$  and a significant nonuniform enhancement for  $2.1 \leq q_\epsilon \leq 2.8 \text{ fm}^{-1}$  relative to HO single-particle values. Within the context of the models discussed, the  $M3$  cross section is suppressed by about a factor of 3. However, we point out that  $M3$  suppression alone is not sufficient to explain the data. The other multipoles contributing in the suppressed region must also be altered. The high- $q$  data, for example, could be consistent with a broadening or shifting of the  $M5$ . The comparisons to theory discussed above have been based on the shapes of the magnetic form factors available from spherical potential models. If these shapes were altered by effects

such as a strong deformation, the quantitative interpretation of the data would be different. At present, however, no available theoretical model is capable of explaining the features displayed by the data.

We acknowledge the assistance and support of our colleagues with great pleasure. In particular, we wish to thank J. Heisenberg for many valuable discussions and ideas. The expert chemical and metallurgical skills of R. H. Condit, W. E. Sunderland, and W. H. Parrish from Lawrence Livermore Laboratory made the measurements discussed here possible. We also thank A. Arima, B. A. Brown, W. Chung, T. W. Donnelly, and E. Moniz for their important theoretical contributions. This research was supported in part by the U. S. Department of Energy, Contract No. EY-76-C-02-3069.\*000, the National Research Council of Canada, and the Deutscher Akademischer Austausch Dienst.

<sup>(a)</sup> Present address: Institute für Kernphysik, Universität Mainz, Mainz, Germany.

<sup>1</sup>F. Ajzenberg-Selove, Nucl. Phys. **A281**, 1 (1977).

<sup>2</sup>W. Bertozzi, M. V. Hynes, C. P. Sargent, C. Creswell, P. C. Dunn, A. Hirsch, M. Leitch, B. Norum, F. N. Rad, and T. Sasanuma, Nucl. Instrum. Methods **141**, 457 (1977); S. Kowalski *et al.*, in *Medium Energy Nuclear Physics with Electron Linear Accelerators*, edited by W. Bertozzi and S. Kowalski, U. S. AEC Report No. TID-24667 (National Technical Information Service, Springfield, Va., 1967), p. 39.

<sup>3</sup>H. Miska, B. Norum, M. V. Hynes, W. Bertozzi, S. Kowalski, F. N. Rad, C. P. Sargent, T. Sasanuma, and B. L. Berman, Bull. Am. Phys. Soc. **23**, 29 (1978), and to be published.

<sup>4</sup>G. A. Peterson, J. B. Flanz, R. S. Hicks, A. Hotta, R. A. Lindgren, H. deVries, D. V. Webb, R. C. York, and C. F. Williamson, Bull. Am. Phys. Soc. **23**, 583 (1978), and to be published.

<sup>5</sup>R. H. Condit, W. H. Parrish, Sr., and W. E. Sunderland, to be published.

<sup>6</sup>R. E. Rand, R. Frosch, and M. R. Yearian, Phys. Rev. **144**, 859 (1966); L. Lapikas, G. Box, and H. deVries, Nucl. Phys. **A253**, 324 (1975).

<sup>7</sup>R. S. Willey, Nucl. Phys. **40**, 529 (1963).

<sup>8</sup>T. W. Donnelly, private communication.

<sup>9</sup>B. S. Reehal and B. H. Wildenthal, Part. Nucl. **6**, 137 (1973); B. A. Brown and W. Chung, private communication.

<sup>10</sup>A. Arima, Y. Horikawa, H. Hyuga, and T. Suzuki, Phys. Rev. Lett. **40**, 1001 (1978).

<sup>11</sup>J. Dubach, private communication.

<sup>12</sup>L. Zamick, Phys. Rev. Lett. **40**, 381 (1978).

<sup>13</sup>B. A. Brown, private communication.

<sup>14</sup>T. W. Donnelly and J. D. Walecka, Nucl. Phys. **A201**, 81 (1973).

<sup>15</sup>P. K. A. deWitt Huberts, L. Lapikas, H. deVries,

J. B. Bellicard, J. M. Cavedon, B. Frois, M. Huet, Ph. Leconte, A. Nakada, Phan Xuan Ho, S. K. Platchkov, and I. Sick, Phys Lett. **71B**, 317 (1977).

## Pion Production in the $^{40}\text{Ar} + ^{40}\text{Ca}$ Reaction at 1.05 GeV/Nucleon

K. L. Wolf,<sup>(a)</sup> H. H. Gutbrod, W. G. Meyer, A. M. Poskanzer, A. Sandoval, R. Stock, J. Gosset,<sup>(b)</sup> C. H. King, G. King, Nguyen Van Sen,<sup>(c)</sup> and G. D. Westfall  
*Lawrence Berkeley Laboratory, Berkeley, California 94720, Gesellschaft für Schwerionenforschung, Darmstadt, West Germany, and Fachbereich Physik, Universität Marburg, Marburg, West Germany*

(Received 20 February 1979)

Pion-production cross sections have been measured for the reaction  $^{40}\text{Ar} + ^{40}\text{Ca} \rightarrow \pi^+ + X$  at a laboratory energy of 1.05 GeV/nucleon. A maximum in the  $\pi^+$  cross section occurs at mid-rapidity, which is anomalous relative to  $p + p$  and  $p + \text{nucleus}$  reactions and compared to many other heavy-ion reactions. Calculations based on cascade and thermal models fail to fit the data.

In high-energy heavy-ion reactions it is generally believed that single-particle inclusive cross sections of  $\pi$ ,  $p$ ,  $d$ ,  $t$ , etc., are dominated by simple factors such as geometry and energy-momentum conservation, and contain little information about the initial "compression" or early "expansion" stages of central or near-central collisions.<sup>1</sup> This may be attributed to the effect of averaging caused by large particle multiplicities, the acceptance of events from all impact parameters, and the rescattering of products due to very short mean free paths. For similar reasons, theoretical models using cascade,<sup>2,3</sup> fire-streak,<sup>4</sup> or hydrodynamic<sup>5</sup> assumptions usually give semiquantitative agreement with particle-inclusive data.<sup>6</sup> Therefore, it is interesting that in the present study of the  $^{40}\text{Ar} + ^{40}\text{Ca}$  reaction at 1.05 GeV/nucleon, the  $\pi^+$  emission pattern is peaked in the mid-rapidity region, which is not predicted by theoretical calculations and is unique compared to  $p + p$  and  $p + \text{nucleus}$  reactions and heavy-ion reactions at lower bombarding energies. Because of this unusual behavior, the possibility must be considered that the structure in the  $\pi^+$  cross section near  $90^\circ$  in the center-of-mass system may be a signature of processes from an early stage of the reaction which has not been fully averaged out.

One can understand how such information might survive in this particular instance for low-energy pions produced in a rather light system. Because of a large energy threshold, pions are produced preferentially in regions of high density and tem-

perature or from particularly violent nucleon-nucleon collisions, with little contribution from spectator deexcitation. Furthermore, since these pion energies near  $90^\circ$  in the c.m. system are well below the  $\Delta(1232)$  resonance energy, it is expected that the mean free path is comparable to the dimensions of the  $^{40}\text{Ar} + ^{40}\text{Ca}$  system, allowing an appreciable amount of unattenuated pion emission.

A beam of  $^{40}\text{Ar}$  ions at 1.05 GeV/nucleon from the Lawrence Berkeley Laboratory Bevalac was used to induce reactions in a 200-mg/cm<sup>2</sup> Ca target. Pions were identified and the energy spectra were measured over a range of 15–95 MeV with a multielement  $dE/dx$  telescope<sup>1</sup> consisting of a 5-mm Si(Li) crystal, and 28- and 42-mm intrinsic germanium crystals with a Si(Li) reject counter. A delayed-coincidence technique was applied to identify stopped  $\pi^+$  by observing the positrons from the subsequent muon decay in the germanium crystals of the detector, from the decay sequence  $\pi^+ \xrightarrow{25 \text{ ns}} \mu^+ \xrightarrow{2.2 \text{ } \mu\text{s}} e^+ + \nu + \bar{\nu}$ . Pion energy spectra were corrected for absorption, multiple scattering, and the inefficiency of detecting the positrons produced in the muon decay. The systematic uncertainty in the  $\pi^+$  cross sections is estimated to be  $\approx 30\%$  with a precision better than 10%. In addition to the pion-inclusive measurements, the associated charged-particle multiplicity was determined on an event-by-event basis, allowing a type of impact parameter selection.<sup>1</sup> The multiplicity was measured with an 80-counter array of plastic scintillators coupled to